Dislocation-Free Island Formation in Heteroepitaxial Growth: A Study at Equilibrium

István Daruka and Albert-László Barabási
Department of Physics, University of Notre Dame, Notre Dame, Indiana 46556
(Received 8 May 1997)

We investigate the equilibrium properties of strained heteroepitaxial systems, incorporating the formation and the growth of a wetting film, dislocation-free island formation, and ripening. The derived phase diagram provides a detailed characterization of the possible growth modes in terms of the island density, equilibrium island size, and wetting layer thickness. Comparing our predictions with experimental results we discuss the growth conditions that can lead to stable islands as well as ripening. [S0031-9007(97)04531-6]

PACS numbers: 68.55.Jk, 68.35.Md

Heteroepitaxial growth of highly strained structures has gained interest lately as it offers the possibility to fabricate nanoscale islands with very narrow size distribution [1]. Typically, H monolayers (ML) of atoms are deposited on a substrate, where the substrate and the deposited film have different equilibrium lattice constants. For small coverage the experiments document the pseudomorphical formation of a wetting film, but after the film reaches a certain critical thickness, H_c, dislocation-free islands form on the substrate. Thanks to their small and uniform size, these islands, coined self-assembling quantum dots (SAQD), are candidates for three dimensional electron confinement [1].

The controlled production of SAQDs for both optical and electronic applications requires a good description of the basic mechanisms determining the size and the distribution of the islands. However, such an understanding is hampered by the coexistence of equilibrium and nonequilibrium effects: while the experimentally well documented existence of a flux independent critical wetting film thickness [2], H_c, is well described by equilibrium theories of heteroepitaxial growth [3], the observed flux and temperature dependence of the island sizes [1] provide direct evidence of nonequilibrium effects contributing to the island formation process [4]. A detailed theory of SAQD formation, incorporating both nonequilibrium and equilibrium effects, is beyond reach at this point. However, since for reversible systems nonequilibrium effects represent the path of the system towards an equilibrium state, an adequate theory of SAQD formation should first provide a detailed description of the equilibrium states supported by the dislocation-free strained system. An important step in this direction was taken by Shchukin *et al.* [5], who found that depending on the material constants and the misfit one can obtain either stable islands, or ripening takes place in the system. However, by neglecting the existence of the wetting layer, their study could not predict the actual growth mode, nor could provide the island density, island size, and the wetting layer thickness as a function of the deposited material, quantities that can be measured experimentally with great accuracy [1].

In this paper we investigate the equilibrium properties of strained heteroepitaxial systems, incorporating the growth of the wetting film, dislocation-free island formation, and ripening. Our results can be summarized in a phase diagram, which not only predicts the main growth modes, but also provides a detailed characterization of the possible phases in terms of the island density, equilibrium island size, and wetting layer thickness. We find that the stability of the islands depends very sensitively on the coverage; i.e., the misfit strain and the coverage have to exceed a critical value for stable islands to exist, and that for *any* misfit there is a second critical coverage beyond which ripening occurs.

Model and free energy.—We consider that H monolayers of atom A with lattice constant d_A are deposited on top of the substrate B with lattice constant d_B, and are allowed to equilibrate. Because of the lattice mismatch, $\epsilon = (d_A - d_B)/d_B$, in equilibrium one expects that a certain fraction of the atoms A forms a wetting film of n_1 monolayers and the rest of the material ($H - n_1$ monolayers) is distributed in 3D islands. We consider that the 3D islands have a pyramidal shape with a fixed aspect ratio, corresponding to a single minima in the Wulff's plot. Neglecting evaporation, the deposited material represents a conserved system in equilibrium with a thermal reservoir; thus the relevant thermodynamical potential density is the free energy per atom, $f = u - Ts$, where u is the internal energy density, T is the temperature, and s is the entropy density of the system. However, one can show that the entropic contribution to f is negligible; thus $f \approx u$, where

$$u(H, n_1, n_2, \epsilon) = E_{\mathrm{ml}}(n_1) + n_2 E_{\mathrm{isl}} + (H - n_1 - n_2) E_{\mathrm{rip}} . \qquad (1)$$

The first term provides the contributions of the n_1 strained overlayers, being an integral over the binding and the elastic energy densities. The energy density of a uniformly strained layer is given by $G = C\epsilon^2 - \Phi_{AA}$, where $-\Phi_{AA}$ is the energy of an AA bond and C is a material constant, being a function of the Young modulus and the Poisson ratio [6]. At the wetting layer-substrate interface atoms have AB bonds with the substrate with a binding energy

 0031-9007/97/79(19)/3708(4)$10.00

$-\Phi_{AB}$, such that $\Delta = \Phi_{AA} - \Phi_{AB} < 0$ (wetting condition). However, due to the short range intermolecular interactions the binding energies of A atoms close to (but not at) the substrate is also modified [3]: as we move away from the substrate, the binding energy density increases from $-\Phi_{AB}$ (in the first monolayer) to its asymptotic value $-\Phi_{AA}$. These intermolecular forces are responsible for the critical layer thickness larger than one monolayer in heteroepitaxy [3]. To include this effect we calculate the total energy stored in the wetting layer as

$$E_{\mathrm{ml}}(n_1) = \int_0^{n_1} dn\{G + \Delta[\Theta(1-n) + \Theta(n-1)e^{-(n-1)/a}]\}, \quad (2)$$

where $\Theta(x) = 0$ if $x < 0$ and $\Theta(x) = 1$ if $x > 0$. The $a = 0$ limit corresponds to the absence of the short range forces. While (2) provides a reasonable fit to the result of Ref. [3], the particular form of (2) does not modify the qualitative behavior of the free energy provided that the binding energy is strictly monotonous and bounded as a function of n.

The second term in Eq. (1) describes the free energy per atom of the pyramidal islands and the island-island interaction [5]

$$E_{\mathrm{isl}} = gC\epsilon^2 - \Phi_{AA} + E_0\left(-\frac{2}{x^2}\ln e^{1/2}x + \frac{\alpha}{x} + \frac{\beta(n_2)}{x^{3/2}}\right), \quad (3)$$

where $x = L/L_0$ is the reduced island size, L_0 being a material dependent characteristic length [5]. Departures from planar geometries can lead to the relaxation of the strain energy. Thus the strain energy density of the islands [first term in Eq. (3)] is lower than that of the compressed wetting layer, this reduction being expressed by the form factor g $(0 < g < 1)$ [5]. The second term stands for the binding energy. The elastic energy of an edge of length L is proportional to $-L\ln L$ [7]; thus the energy density is $\sim -\ln L/L^2$, accounting for the first of the three terms in the parentheses. The interaction of the homoepitaxial and heteroepitaxial stress fields leads to a cross term $-\epsilon/L \sim -\epsilon/x$. Furthermore, the facet energy is proportional to the area of the facet, L^2, giving the energy density as $\sim 1/L \sim 1/x$. The cross term and the facet energies are combined in the second term in the parentheses of Eq. (3), α/x, with $\alpha = p(\gamma - \epsilon)$, where p and γ are material constants describing the coupling between the homoepitaxial and heteroepitaxial stress fields (also function of the island geometry) and the extra surface energy introduced by the islands, respectively. Finally, since the stress fields of the individual islands overlap, there is island-island interaction, described by the last term in the parentheses of Eq. (3), where $\beta(n) = b\epsilon^2 n^{3/2}$ [5]. This can be expressed in terms of the average island spacing $d = 1/\sqrt{\rho_{\mathrm{isl}}}$ and the reduced island size x, giving the interaction term as $\sim(x/d)^3$, corresponding to the dipole-dipole interaction between the islands [8]. The energy terms appearing in Eq. (3) are scaled by the characteristic energy E_0 set by the edge energy of an island of size L_0. We also scale C, Φ_{AA}, and Φ_{AB} by E_0; thus the results are independent of the numerical value of E_0.

The total elastic energy density of the ripened islands can be obtained from (3) by taking the limit $x \to \infty$, providing $E_{\mathrm{rip}} = gC\epsilon^2 - \Phi_{AA}$, which is multiplied by the total number of atoms stored in the ripened islands, $(H - n_1 - n_2)$.

Phase diagram.—Equations (1)–(3) define the free energy of the wetting film and 3D pyramidal islands, whose minima determine the equilibrium properties of the system. Consequently, we have to minimize f in respect to n_1, n_2, and x. The growth modes (phases) provided by the minimization process, as a function of the two most relevant experimental parameters, the amount of the deposited material H and the misfit ϵ, are summarized in the phase diagram shown in Fig. 1. In the following we discuss the properties of the phases predicted by our analysis.

(i) FM phase.—If $H < H_{c_1}(\epsilon)$, the deposited material contributes to the pseudomorphic growth of the wetting film and islands are absent, reminiscent of the Frank

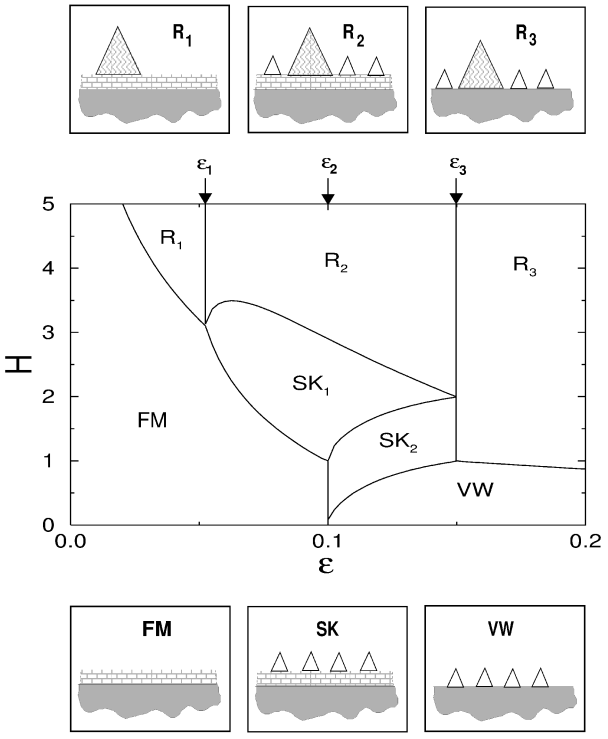

FIG. 1. Equilibrium phase diagram in function of the coverage H and misfit ϵ. The small panels on the top and the bottom illustrate the morphology of the surface in the six growth modes. The small empty islands indicate the presence of stable islands, while the large shaded one refers to ripened islands. The phases are separated by the following phase boundary lines: $H_{c_1}(\epsilon)$: FM-R_1, FM-SK_1; $H_{c_2}(\epsilon)$: SK_1-R_2; $H_{c_3}(\epsilon)$: SK_2-SK_1; $H_{c_4}(\epsilon)$: VW-SK_2, VW-R_3. The parameters used to obtain the phase diagram are $a = 1$, $C = 40E_0$, $\Phi_{AA} = E_0$, $\Phi_{AB} = 1.27E_0$, $g = 0.7$, $p = 4.9$, $\gamma = 0.3$, and $b = 10$.

van der Merve (FM) growth mode. The free energy has its minima at $n_2 = 0$ and $n_1 = H$, indicating that the thickness of the wetting layer coincides with the nominal thickness of the deposited material, H [see Fig. 2(a)]. The growth of the wetting layer continues until H reaches a critical value, $H_{c_1}(\epsilon)$, the phase boundary between the FM and the R_1 or SK_1 phase.

(ii) R_1 phase.—Above $H_{c_1}(\epsilon)$, for $0 < \epsilon < \epsilon_1$, the free energy develops a new minima at $n_2 = 0$ and $0 < n_1 < H$. Consequently, after the formation of a wetting layer of $n_1 = H_{c_1}(\epsilon)$ monolayers, the excess material $(H - n_1)$ contributes to the formation of ripened islands. The free energy decreases monotonically for large x; thus there is a tendency to accumulate all available material $[H - H_c(\epsilon)]$ in as large islands as possible. These ripened islands, being infinitely large, have zero density.

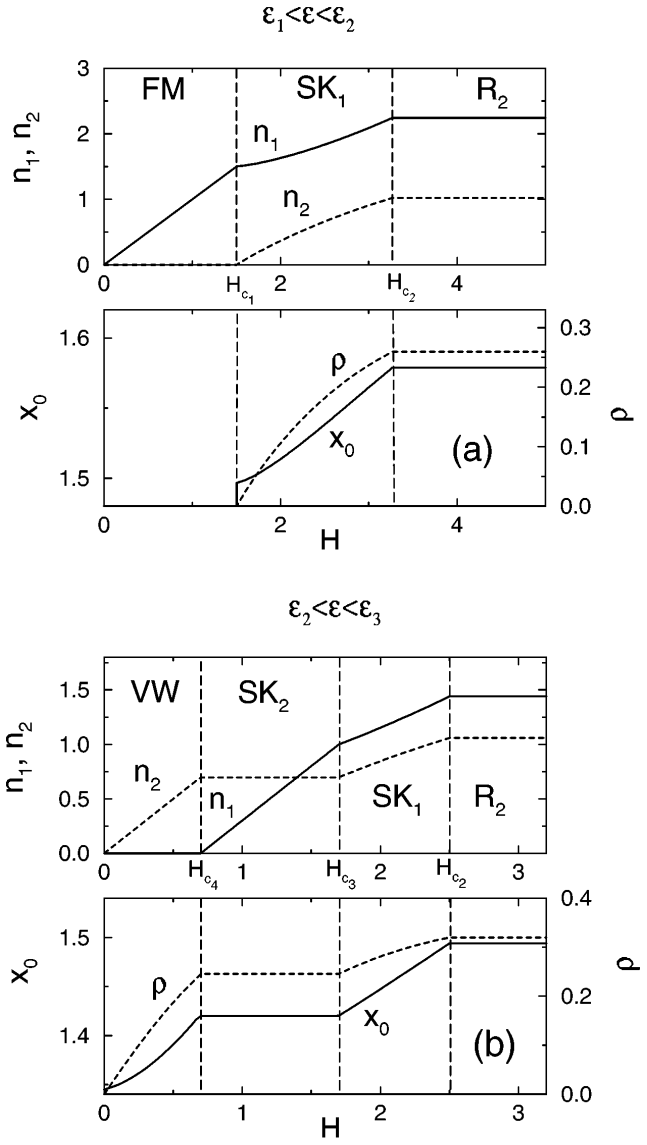

FIG. 2. (a) Wetting film thickness (n_1), island coverage (n_2) (top), island size (x_0), and island density (ρ) (bottom) as a function of H for $\epsilon = 0.08$. At H_{c_1} there is a transition from the FM to the SK_1 phase, the island size jumping discontinuously. In the R_2 phase, present for $H > H_{c_2}$, ripening takes place; (b) same as (a) but for $\epsilon = 0.12$. At H_{c_4} there is a transition from the VW to the SK_2 phase followed by the SK_1 phase at H_{c3}. And finally, at H_{c_2} the system reaches the R_2 phase.

(iii) SK_1 phase.—Above $H_{c_1}(\epsilon)$, for $\epsilon_1 < \epsilon < \epsilon_2$, the free energy develops a new minima at nonzero n_1 and n_2, such that $n_1 + n_2 = H$, i.e., the deposited material (H) is distributed between n_1 layers, forming the wetting film, and finite islands, whose total mass is n_2 [see Fig. 2(a)], similar to the Stranski-Krastanow (SK) growth mode. At $H_{c_1}(\epsilon)$ the equilibrium island size jumps from zero (in the FM phase) to some finite $x_0(H, \epsilon)$ value. Naturally, within the SK_1 phase, n_1, n_2, x_0, and the island density ρ are continuous functions of H and ϵ. As Fig. 2(a) indicates, with increasing H, ρ increases from zero at H_c to a finite value. Because of the island-island interaction, the wetting layer continues to grow sublinearly.

(iv) R_2 phase.—In this phase, the free energy surface has a minima at $0 < n_1 < H$, $0 < n_2 < H$, such that $H - n_1 - n_2 > 0$, indicating that the deposited material is distributed between a wetting film, finite islands, and ripened islands $(H - n_1 - n_2)$. The finite islands formed in the SK_1 phase are preserved [see Figs. 2(a) and 2(b)], being stable in respect to ripening. Thus finite and ripened islands coexist in the R_2 phase.

(v) VW phase.—For large misfit $(\epsilon > \epsilon_2)$ and for small coverages $[H < H_{c_4}(\epsilon)]$, the free energy has its minima at $n_2 = H$ and $n_1 = 0$, indicating that all the deposited material is accumulated in finite islands. Because of the large misfit, in this phase the wetting film is absent and the islands form directly on the substrate, similar to the Volmer-Weber (VW) growth mode.

(vi) SK_2 phase.—For $\epsilon_2 < \epsilon < \epsilon_3$, increasing H, at $H_{c_4}(\epsilon)$, we reach the SK_2 phase. The behavior of the system is different from the SK_1 growth mode: at the H_{c_4} boundary we have islands formed in the VW mode. As Fig. 2(b) indicates, in the SK_2 phase the island density and the island size remain unchanged, and a wetting film starts forming. This process continues until a full monolayer is completed, at which point we enter the SK_1 phase. In contrast with the SK_1 phase, in the SK_2 phase the formation of further islands is suppressed until the one monolayer thick wetting layer is completed.

(vii) R_3 phase.—In this phase, present for $\epsilon > \epsilon_3$ and for $H > H_{c_4}$, the free energy has its minima at $n_1 = 0$ and $0 < n_2 < H$, indicating the formation of ripened islands. The formation of stable islands is suppressed, and all the material deposited after H_{c_3} contributes only to the ripened islands, coexisting with the stable islands formed in the VW growth mode. However, in contrast to R_2, in R_3 a wetting film is absent.

Comparison with experiments.—A quantitative comparison of the phase diagram with the experiments requires the knowledge of the material constants in (1)–(3), which determine the precise value of ϵ_1, ϵ_2, ϵ_3, and the location of the lines in the phase diagram. However, the

topology of the phase diagram is *material independent*, as long as the SK phase is supported by the system. This robustness of the phase diagram implies that in equilibrium these are the *only phases* supported by the free energy (1)–(3).

During ripening, when the island size reaches a certain critical size, dislocation formation relaxes the strain energy of the islands, allowing the fast growth of dislocated islands. Furthermore, many experiments were done at large enough flux so that one suspects that equilibrium has not been reached yet. Finally, nucleation barriers might slow down the convergence to an equilibrium state, trapping the system in metastable states [9].

Our analysis indicates that for strain induced island formation there is a critical strain, ϵ_1, such that for any $\epsilon > \epsilon_1$ *stable islands are possible*. A second important consequence is that for any ϵ, for *large enough coverage ripening will occur*. Thus in order to obtain stable islands, H must *not* exceed the boundary of the ripening phase. This result can provide an efficient test of our predictions: in systems where ripening has been observed, we predict that ripening can be avoided by choosing a smaller coverage H.

The formation of the pseudomorphic wetting layer for small H and ϵ has been documented in various systems, being a general feature of strained layer formation. Detailed measurements on InAs/GaAs have shown that the transition from the FM to the SK_1 phase occurs at $H_{c_1} \simeq 1.7$ ML, independent of the deposition rate [2], indicating that its origin is thermodynamic rather than dynamic [10]. Furthermore, recent investigations have measured the strain dependence of H_{c_1}: results on GeSi grown on Si and AlInAs grown on AlGaAs have indicated that the critical wetting layer thickness decreases with increasing misfit [11], in agreement with the decreasing tendency of the H_{c_1} phase boundary (Fig. 1).

After the critical thickness has been reached, rapid formation of uniform islands is observed [1]. Studies of InAs grown on GaAs indicate that near H_{c_1} the island density increases as $\rho \sim [H - H_c(\epsilon)]^\gamma$ [12], signaling a second order phase transition in the system. Furthermore, we find that in the close vicinity of H_{c_1} we have $\gamma = 1$, i.e., the island density increases linearly with $(H - H_{c_1})$. However, for large $(H - H_{c_1})$ the island-island interaction leads to a sublinear increase in the density. Indeed, Miller *et al.* [12] found that after stopping deposition the system had a transient regime, after which it equilibrated. The *equilibrated* island density *increased linearly* with the coverage, in agreement with our prediction $\gamma = 1$. Furthermore, a linear expression provides an excellent fit near H_{c_1} to the data of Ref. [12] as well.

We find that unlike ρ, the equilibrium island size does not increase continuously near H_{c_1}, but it *jumps discontinuously* from zero to $x_0(\epsilon, H_{c_1})$. This is again in agreement with the experiments, since once islands form, they reach a well defined size and small islands are rather rare [1,13]. Also, the experiments indicate that while an increasing H does modify the equilibrium island size, this change is not significant, but most of the newly deposited material contributes to the formation of new islands [1], again in agreement with slowly changing x_0 and rapidly increasing ρ in Fig. 2.

Finally, the phase diagram indicates that the stability of the islands depends on the coverage: *independent of* ϵ, *for large* H ripening should take place in the system. Indeed, for CdSe grown on ZnMnSe repeated antiferromagnetic scans of the same sample made at 48 hour intervals indicate that some islands ripen at the expense of others, and the overall island density decreases with time [14]. However, the fact that the stable islands do not coexist with the ripened ones, as expected in the R_2 and R_3 phases, suggests that these experiments were performed either at the FM and R_1 phase boundary, or dislocations relax the ripened islands. The coexistence of stable and ripened islands is documented for Ge grown on Si [13], that, together with the evidence of a wetting film in this system, indicates that these experiments are done at the border of the SK_1 and R_2 phases, and consequently stable SK islands are allowed for smaller coverages, assuming that dislocations are not the sole origin of the ripened islands.

We have benefited from useful comments and discussions with J. K. Furdyna and J. Tersoff.

[1] For a recent review, see W. Seifert *et al.*, J. Progr. Crystal Growth Charact. Mater. **33**, 423 (1996); P. M. Petroff and G. Medeiros-Ribeiro, MRS Bull. **21**, 50 (1996).
[2] J.-M. Gerard, in *Confined Electrons and Photons*, edited by E. Burstein and C. Weisbuch (Plenum Press, New York, 1995).
[3] J. Tersoff, Phys. Rev. B **43**, 9377 (1991); C. Roland and G. H. Gilmer, Phys. Rev. B **47**, 16 286 (1993).
[4] A.-L. Barabási, Appl. Phys. Lett. **70**, 2565 (1997); B. G. Orr *et al.*, Europhys. Lett. **19**, 33 (1992).
[5] V. A. Shchukin *et al.*, Phys. Rev. Lett. **75**, 2968 (1995).
[6] L. D. Landau and E. M. Lifshitz, *Theory of Elasticity* (Pergamon Press, Oxford, 1986).
[7] V. I. Marchenko, Sov. Phys. JETP **54**, 605 (1981).
[8] J. M. Rickman and D. J. Srolovitz, Surf. Sci. **284**, 211 (1993).
[9] D. Jesson *et al.*, Phys. Rev. Lett. **77**, 1330 (1996).
[10] I. Daruka and A.-L. Barabási, Phys. Rev. Lett. **78**, 3027 (1997).
[11] G. Abstreiter *et al.*, Semicond. Sci. Technol. **11**, 1521 (1996).
[12] D. Leonard *et al.*, Phys. Rev. B **50**, 11 687 (1994); N. P. Kobayashi *et al.*, Appl. Phys. Lett. **68**, 3299 (1996); M. S. Miller *et al.*, Solid State Electron. **40**, 609 (1996).
[13] T. I. Kamins, E. C. Carr, R. S. Williams, and S. J. Rosner, J. Appl. Phys. **81**, 211 (1997).
[14] S. H. Xin *et al.*, Appl. Phys. Lett. **69**, 3884 (1997).